

# Inner Structure of Inhomogeneous Copolymer Latex Particles

Havazelet Bianco, Moshe Narkis, and Yachin Cohen\*

Department of Chemical Engineering, Technion-Israel Institute of Technology, Haifa 32000, Israel

Received November 5, 1996; Revised Manuscript Received February 28, 1997

**ABSTRACT:** A small-angle X-ray scattering (SAXS) study of a model copolymer latex, composed of styrene and pentabromobenzyl acrylate (PBBA, 40 wt %), is presented. The contrast variation method employed in this study was shown to be a sensitive probe for inhomogeneity in the particles. The separation of the homogeneous function allows direct calculation of the size distribution of the spherical particles (volume average diameter,  $26.7 \pm 1.3$  nm). The SAXS analysis reveals a particle's inner structure described as a continuous copolymer phase, of composition being slightly richer in PBBA, within which domains of polystyrene are randomly distributed. The volume fraction of the polystyrene domains was estimated as 11 vol % and their characteristic length as 5.1 nm.

## Introduction

Emulsion copolymerization has been widely used in the industry for production of polymeric materials with tailored properties. It is well-known that the level of homogeneity of the copolymer is an important factor determining the physical properties of the material.<sup>1</sup> Heterogeneity on the molecular level, arising both from the statistical nature of the copolymerization process and from the composition drift occurring along the reaction course, have been extensively studied both from the theoretical<sup>2,3</sup> and the experimental<sup>4–7</sup> points of view. Yet, remarkably little quantitative information is available on heterogeneity on the colloidal scale, determining the morphology of a latex particle.

Small-angle scattering techniques, capable of detecting nano-scale heterogeneity within a latex particle, can be useful tools for structural analysis. The contrast variation method<sup>8,9</sup> is particularly suitable for cases where no *a priori* information related to the particle's inner structure is available. As a first step, a straightforward indication of a particle heterogeneity can be obtained by recording several scattering curves, each having a different scattering density of the dispersing medium. The scattering curves of homogeneous systems are essentially independent of contrast, simply scaling as the contrast is changed. If, however, any inner structure exists in the colloidal particles, changes in contrast will alter the angular dependence of the scattered intensity. A quantitative analysis of these changes allows better determination of the particle shape and, at the same time, yields some quantitative measures of its inner structure.

In a recent publication,<sup>10</sup> a model for the scattering pattern of a dilute dispersion of particles having an irregular inner structure, made of randomly distributed two phases, was presented. In the present study, this model is used in small-angle X-ray scattering (SAXS) experiments for quantitative determination of the inner structure of a model copolymer latex, composed of styrene and pentabromobenzyl acrylate (PBBA). These copolymers have a single glass transition temperature,<sup>11</sup> i.e., homogeneous on the macroscopic level. Yet, kinetic measurements showed that the chemical composition slightly changes during the reaction course, which might result in heterogeneity on a nanometric scale.

**Table 1: Polymerization Recipe**

component	quantity (g)
water	1620
styrene	48
PBBA	32
K <sub>2</sub> S <sub>2</sub> O <sub>8</sub>	4.5
SDS	2.7
Triton X-100	27
KOH	0.675

## Experimental Section

**Materials.** The styrene monomer (Riedel de Haën) was washed with a 5 wt % sodium hydroxide aqueous solution. The PBBA monomer (Bromine Compounds Ltd., Israel, technical grade) was purified by recrystallization from hot toluene. All the other chemicals were of analytical grade, used as received. A mixed surfactant system of sodium dodecyl sulfate (anionic, BDH) and Triton X-100 (nonionic, Bio LAB Ltd.) was employed. Potassium persulfate, K<sub>2</sub>S<sub>2</sub>O<sub>8</sub> (Riedel de Haën) was used as an initiator and potassium hydroxide (Frutarom, Israel) as a pH regulator. Water was deionized and distilled.

**Polymerization.** Emulsion copolymerization of styrene with PBBA was previously described by Yuan et al.<sup>11</sup> Emulsion polymerization was carried out in a 2 L stirred glass reaction vessel, at a constant bath temperature of 70 °C, under nitrogen. The quantities of the ingredients are shown in Table 1. The latex was prepared by a dropwise addition procedure of the monomer mixture, at a rate of about 1 g/min, to the reaction vessel containing all other ingredients. The polymerization process was continued for 4 h after the monomer mixture addition, to complete the reaction.

**Characterization.** The solid copolymer was recovered by drying the latex, extracting the surfactants with hot methanol and distilled water, drying in a vacuum oven at 60 °C, and finally hot-pressing in a compression mold. Density measurements were performed according to ASTM D792 (method A). The density of the copolymer was found to be 1.41 g/cm<sup>3</sup>.

Latex particles were observed with a JEOL 2000FX transmission electron microscope (TEM) at an acceleration voltage of 100 kV. Samples were prepared by drying a drop of diluted latex on a carbon-coated copper grid.

SAXS measurements were performed with Cu K $\alpha$  radiation using a compact Kratky camera having a linear position sensitive detector system (Raytech) with pulse-height discrimination and a multichannel analyzer (Nucleus). The entrance slit to the collimation block was 10  $\mu$ m, and the slit length delimiters were set at 15 mm. The sample to detector distance was 26.4 cm. Latex samples were placed in cylindrical quartz cells (A. Paar Co., 1 mm path length).

The electron density of the dispersing medium  $\rho_m$  (e/nm<sup>3</sup>) was varied by means of adding sucrose to the latex samples, which were diluted to about 1.5 vol %.  $\rho_m$  was calculated using the equation given by Digenouts and Ballauff:<sup>12</sup>

\* Author to whom correspondence should be addressed.

© Abstract published in *Advance ACS Abstracts*, August 1, 1997.

$$\rho_m = 332.79 + 1.2827c \quad (1)$$

where  $c$  is the weight percentage of sucrose in the solution.

The sample temperature was kept at 25 °C by means of a temperature controller (A. Paar Co.). Primary beam intensities were determined using the moving slit method of Kratky and Stabinger<sup>13</sup> and subsequently using a thin quartz monitor as a secondary standard. The scattering curves, as a function of the scattering vector  $h = 4\pi \sin \theta / \lambda$  (where  $2\theta$  and  $\lambda$  are the scattering angle and the wavelength, respectively), were corrected for counting time and for sample absorption. The constant background was determined separately for each curve using the Porod law and subtracted.

### Modeling of the SAXS Intensities

The scattering intensity from a dilute system of particles of identical shape (which is overall isotropic) can be regarded as the sum of the intensities scattered by the individual particles. In the most general form, the total scattering intensity per unit volume of sample  $i(h)$ , normalized to the scattering intensity of a single electron, is given by<sup>14–16</sup>

$$i(h) = \varphi \int_0^\infty \frac{f_v(R)}{V_0(R)} \langle F(\underline{h}, R) F^*(\underline{h}, R) \rangle dR \quad (2)$$

where  $\varphi$  is the volume fraction of the particles in the sample,  $f_v(R)$   $dR$  is the volume of particles having a size between  $R$  and  $R + dR$  per total volume of particles,  $F(\underline{h}, R)$  is the structure factor of a single particle having size  $R$  and volume  $V_0(R)$ :

$$F(\underline{h}, R) = \int_{V_0} [\rho(\underline{r}) - \rho_m] e^{-i\mathbf{h} \cdot \underline{r}} d\underline{r} \quad (3)$$

where  $F^*(\underline{h}, R)$  is its complex conjugate,  $\rho(\underline{r})$  is the local electron density, and  $\langle \rangle$  represents averaging over all possible orientations.

If the chemical composition is identical for all particles, the scattering intensity can be split into three contrast-independent “basic functions”:<sup>8,9</sup> the homogeneous part  $i_h(h)$  determined by the particle shape, the heterogeneous part  $i_{ih}(h)$ , and the cross term  $i_i(h)$ :

$$i(h) = (\Delta\rho)^2 i_h(h) + (\Delta\rho) i_{ih}(h) + i_i(h) \quad (4)$$

where the contrast is defined as  $\Delta\rho = \bar{\rho} - \rho_m$  and the average density  $\bar{\rho}$  is given by

$$\bar{\rho} = \frac{1}{V_0} \int_{V_0} \rho(\underline{r}) d\underline{r} \quad (5)$$

Often actual data is acquired using an incident beam having a specific geometry (i.e., slit). In this case the measured (so-called smeared) intensity  $i_s(h)$  is related to the theoretical intensity by the following integral:<sup>14,15</sup>

$$i_s(h) = \int_{-\infty}^{\infty} P(t) i(\sqrt{h^2 + t^2}) dt \quad (6)$$

where  $P(t)$  is the shape of the beam. Since eq 6 describes a linear operator, then eq 4 is equally valid for “smeared” intensities.

### Results and Discussion

The smeared SAXS intensities measured at different contrasts are displayed in Figure 1. As can be seen, changes in the contrast affect both the intensity and the angular dependence of the scattered radiation, indicating inhomogeneity of the latex particles. The TEM micrographs, such as the one shown in Figure 2, reveal the spherical shape and the size polydispersity of the latex particles but do not show any further structural details. Thus, additional information related to the

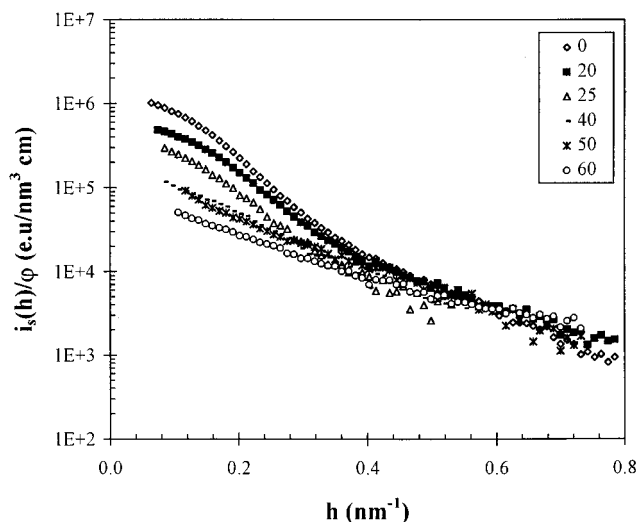


**Figure 1.** Smeared SAXS scattering intensities obtained from 1.5 vol % latex at different contrasts. Legends indicate the weight percentage of sucrose in the solution.

particles' inner structure is most easily obtained from the basic functions.

The forward scattering  $i_s(0)$ , determined for each curve separately using a Guinier plot, is plotted in Figure 3, vs the electron density of the dispersing medium. The average density, determined from the minimum point of that plot (which corresponds to the match point, where  $\bar{\rho} = \rho_m$ ), was found to be 405.6 e/nm<sup>3</sup>. Note that the minimum forward scattering does not vanish. This indicates that the average density is not identical for all particles.<sup>17–19</sup> An estimate for the width of the average density distribution can be obtained from the minimum value of  $i_s(0)$ .<sup>17,18</sup> Since, however, the particles are relatively large, the uncertainty in the extrapolated values  $i_s(0)$ , which are more pronounced near the match point, might lead to a poor approximation. In the following section an alternative procedure that may be more accurate for large particles is proposed.

The basic equation of the contrast variation method (eq 4) can be rewritten in the form

$$i(h, \rho_m) = \rho_m^2 I_h(h) + \rho_m I_{ih}(h) + I_i(h) \quad (7)$$

where the three  $\rho_m$ -independent functions  $I_h(h)$ ,  $I_{ih}(h)$ , and  $I_i(h)$  are defined, using eqs 4 and 7, as

$$I_i(h) = \sum_k [\bar{\rho}_k^2 i_h(h, R_k) + \bar{\rho}_k i_{ih}(h, R_k) + i_i(h, R_k)] \quad (8a)$$

$$I_{ih}(h) = -\sum_k [2\bar{\rho}_k i_h(h, R_k) + i_{ih}(h, R_k)] \quad (8b)$$

$$I_h(h) = \sum_k i_h(h, R_k) \quad (8c)$$

where  $R_k$  is the size of the  $k$ th particle and  $\bar{\rho}_k$  its average density. As  $i_{ih}(0) = i_i(0) = 0$ , extrapolation of these functions to  $h = 0$  yields two measures of the average density:

$$\langle \bar{\rho}_k \rangle \equiv \frac{\sum_k \bar{\rho}_k V_0^2(R_k)}{\sum_k V_0^2(R_k)} = -\frac{I_{ih}(0)}{2I_h(0)}$$

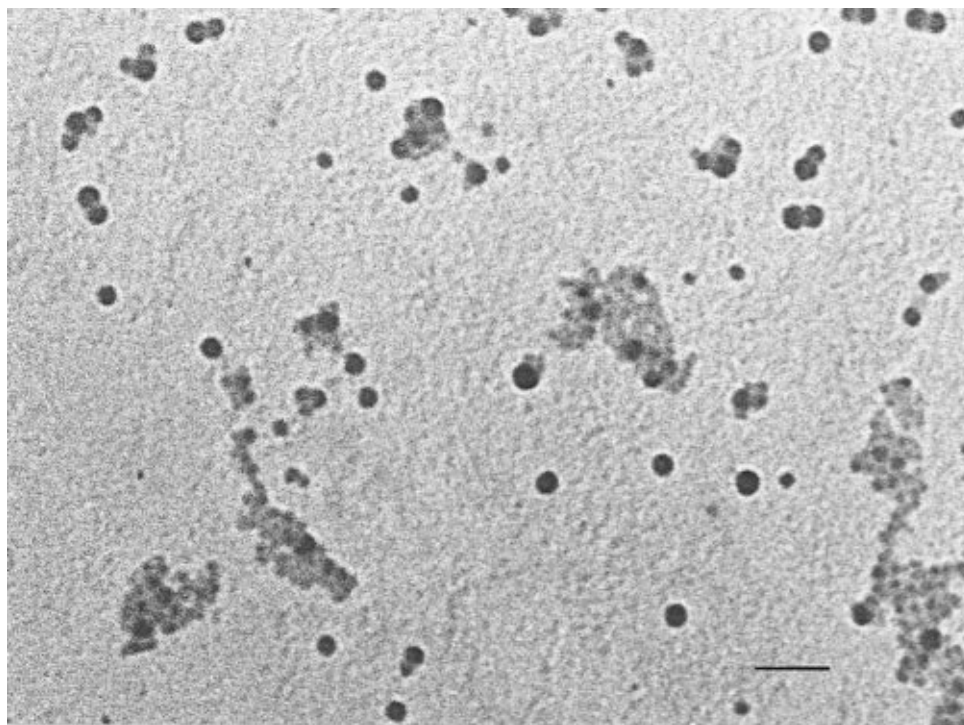


**Figure 2.** TEM micrograph of the styrene/PBBA copolymer latex particles. Bar indicates 100 nm.

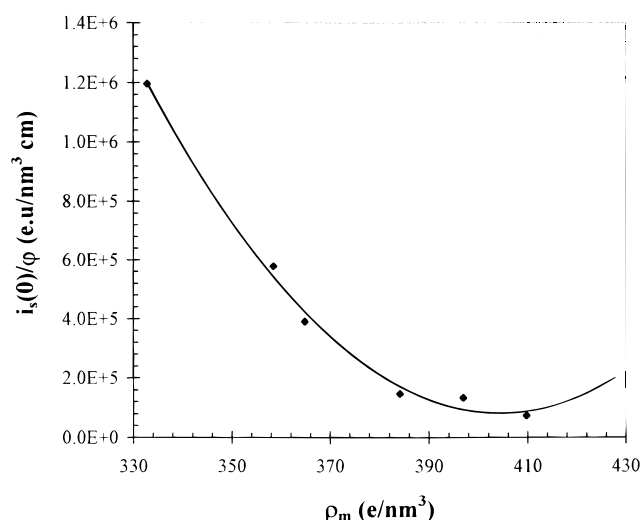


**Figure 3.** Calculation of the average density using the contrast variation method. The forward scattering vs electron density of the medium.

$$\langle \bar{\rho}_k^2 \rangle \equiv \frac{\sum_k \bar{\rho}_k^2 V_0^2(R_k)}{\sum_k V_0^2(R_k)} = \frac{I_i(0)}{I_h(0)} \quad (9)$$

where  $V_0(R_k)$  is the volume of a particle of size  $R_k$ . The ratio  $\langle \rho_k \rangle / (\langle \bar{\rho}_k^2 \rangle)^{1/2}$  can be used as an estimate of the width of the average density distribution.

The whole set of experimental data was used for the calculation of the functions  $I_h(h)$ ,  $I_{ih}(h)$ , and  $I_i(h)$  of eq 7. For each experimental point  $h_i$ , a multivariable linear regression procedure was employed, using the six known values of  $\rho_m$  (and  $\rho_m^2$ ) as the independent parameters. The functions  $I_h(h)$ ,  $I_{ih}(h)$ , and  $I_i(h)$  obtained by this procedure were then extrapolated to zero angle by the Guinier function. This procedure yields more accurate evaluation of the low-angle region of the

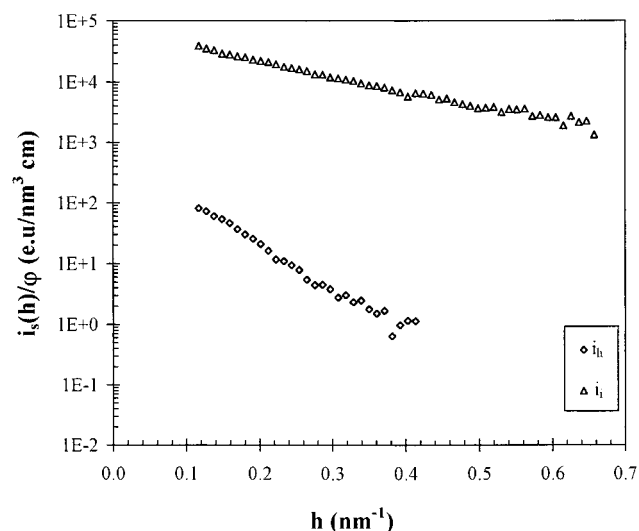


**Figure 4.** The calculated smeared homogeneous and heterogeneous basic functions.

derived functions and hence of their extrapolation to zero angle. From eq 9, values of  $\langle \rho_k \rangle = 403.4$  and  $(\langle \bar{\rho}_k^2 \rangle)^{1/2} = 427.9$  e.u./nm<sup>3</sup> were obtained, i.e., about 6% difference between the two measures of the average density.

As a first assumption, the influence of the average density distribution was neglected. From the measured ("slit-smeared") scattering patterns at different contrasts, the smeared basic functions were calculated. For this purpose, a regression procedure was applied to eq 4, using  $\bar{\rho} = 403.4$  e/nm<sup>3</sup> with  $\Delta\rho_i$  and  $\Delta\rho_i^2$  as the regression parameters.

The homogeneous function  $i_{hs}(h)$ , calculated by this procedure, is displayed in the lower curve of Figure 4. This reflects only the shape and size of particles. The curve does not exhibit any minima or maxima, due to polydispersity of the latex particles and the effect of the finite dimensions of the incident beam. Since the shape of the latex particles is known to be spherical, the

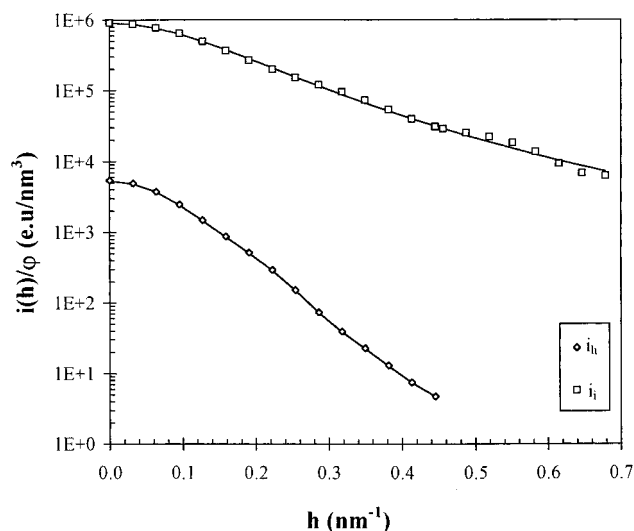


**Figure 5.** Desmeared homogeneous and heterogeneous basic function. Solid lines represent the theoretical intensities.

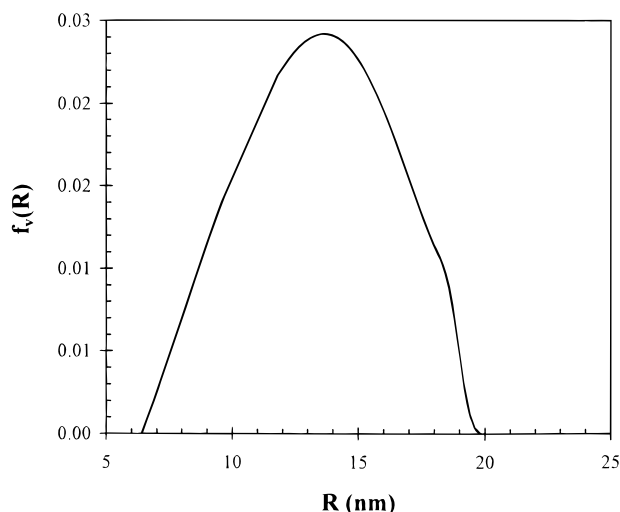


**Figure 6.** Volume distribution of the latex particles, calculated using ITP.

homogeneous part of the scattering curve in polydispersed systems is given by<sup>14,16</sup>

$$i_h(h) = \frac{4\pi}{3} \varphi \int_0^\infty f_v(R) R^3 \Phi^2(hR) dR \quad (10)$$

where  $\Phi(hR)$  is the shape factor:

$$\Phi(hR) = 3 \frac{\sin(hR) - hR \cos(hR)}{(hR)^3} \quad (11)$$

The correction for the dimensions of the primary beam (length and width) and the calculation of size distribution were carried out by the method of indirect Fourier transformation of Glatter,<sup>20–22</sup> using the program ITP. The desmeared intensity  $i_h(h)$  is shown in the lower curve of Figure 5, together with the curve obtained by the transformation procedure (solid line). This procedure yields the size distribution displayed in Figure 6, for whom the volume average diameter is  $26.7 \pm 1.3$  nm and the number average diameter is  $22.6 \pm 1.1$  nm. For comparison, the number average diameter determined from the TEM micrograph (Figure 2) was found to be 23.5 nm.

The calculated (smeared) heterogeneous function  $i_s(h)$  is displayed in the upper curve of Figure 4, and the

desmeared function  $i_i(h)$  is shown in the upper curve in Figure 5. Various structural models, describing a radial distribution of the electron density within the latex particle, can be proposed. These include core-shell structure, multilayer structure (reflecting both composition changes and the adsorbed surfactant layer), and gradual changes in electron density in the radial direction. Test calculations have shown that none of these models could give a reasonable fit to the experimental data. A different type of heterogeneity is an irregular inner structure, namely two phases that are randomly distributed within the particle. The scattering pattern of spherical particles having an irregular inner structure was recently presented<sup>10</sup> in a form amenable for analysis using the contrast variation method. According to that model, the heterogeneous part of the scattering curve may be represented as

$$i_i(h) = 8\pi\xi^3 \varphi \frac{\varphi_1(1 - \varphi_1)(\rho_1 - \rho_2)^2}{(1 + H^2\xi^2)^2} \quad (12)$$

where  $\rho_1$  and  $\rho_2$  are the electron densities of phases 1 and 2, respectively,  $\varphi_1$  is the volume fraction of phase 1 with respect to the particle volume,  $\xi$  is the characteristic length of the inner structure. The derivation of eq 12<sup>10</sup> resulted from the application of the model of Debye, Anderson, and Brumberger<sup>23</sup> for a random two-phase structure to a system of particles with a random two-phase inner structure dispersed in a surrounding medium. It is applicable for values of the scattering vector on the order of  $1/\xi$  or larger. The desmeared function  $i_i(h)$ , shown in the upper curve in Figure 5, could be easily fit by this model, as shown by the solid line. The fit yields a value of  $\xi = 4.68$  nm for the characteristic length of the inner structure.

The composition of the two phases within the particles cannot be determined directly from scattering measurements. However, some insight may be obtained by evaluating specific situations. The mean-squared density fluctuations within the particles  $\eta^2$  can be obtained from the invariant of the total scattering pattern at the match point. This equals the invariant of the inhomogeneous function  $i_i(h)$  in eq 4, denoted  $Q_i \equiv (1/2\pi^2) \int_0^\infty i_i(h) h^2 dh$ . The invariant for a three-phase system has been described by Wu.<sup>24</sup> For a dilute system, where the volume fraction of the dispersing medium is nearly unity, the mean-squared fluctuations are given by the following:

$$\overline{\eta^2} = \varphi_1(1 - \varphi_1)(\rho_1 - \rho_2)^2 = Q_i/\varphi \quad (13)$$

One might suspect that each monomer was polymerized separately, leading to the formation of two phases of the immiscible homopolymers. For this situation, the value of  $\eta^2$ , calculated from the composition and the electron densities of the pure components ( $\varphi_1 = 0.77$  and  $\rho_1 = 339.8$  e/nm<sup>3</sup> for the PS phase and  $\rho_2 = 664.8$  e/nm<sup>3</sup> for the poly(PBBA) phase) should be 18 560 e.u./nm<sup>6</sup>. From the invariant of the heterogeneous function, a value of  $\eta^2 = 499.4$  e.u./nm<sup>6</sup> is obtained, which is more than an order of magnitude smaller. Thus, it has been concluded that intermixing of the components does exist. However, although the value of the average density  $\bar{\rho} = \varphi_1\rho_1 + (1 - \varphi_1)\rho_2$  is known, SAXS analysis cannot

give a unique solution for  $\rho_1$ ,  $\rho_2$ , and  $\varphi_1$  unless one of the parameters can be determined by other means.

Due to the statistical nature of the random copolymerization reaction, each copolymer chain consists of sequences of various lengths of the repeating units, where the mean sequence length of each component is determined by the overall copolymer composition. Small-angle scattering techniques are not sensitive to heterogeneity on the molecular level.<sup>15</sup> Yet, if long sequences of one of the monomers are formed, they might phase-separate and form a discrete phase, having a different electron density than the surrounding copolymer. Thus, phase separation might be an inherent property of the copolymer, and it is likely that the discrete phase mainly contains styrene segments, the major component in the studied system. Another possibility is that long sequences are formed as a result of composition drifts. In a batch reaction, the more reactive monomer disappears faster, leaving a higher concentration of the less reactive monomer which will be polymerized later in the cycle. The composition of the formed copolymer obviously changes in the opposite direction. Copolymers produced by a semibatch reaction, like the one in the present study, are expected to be more homogeneous, since the continuous feed of the monomer mixture minimizes composition drifts. However, once the monomer supply is ceased, composition drift within the monomer-swollen particles are inevitable. The reactivity ratios of PBBA and styrene are not known, but the kinetic data measured by Yuan et al.<sup>11</sup> suggest that PBBA is more reactive. Thus, composition drifts are also expected to induce longer styrene sequences at high conversions.

Although it is hard to decide which one of the two possible mechanisms dictates the phase separation, they both lead to the same description: a major phase of PBBA/styrene copolymer and a minor phase of polystyrene. The SAXS analysis results can now be re-examined by setting a value of  $\rho_1 = 339.8 \text{ e/nm}^3$  for the polystyrene phase, which further allows direct calculation of the other parameters. This yields values of  $\varphi_1 = 0.11 \pm 0.018$  and  $\rho_2 = 411.2 \text{ e/nm}^3$ . Namely, the polystyrene phase is indeed the minor one, occupying 11 vol % of the particle, and the major phase has a slightly higher electron density than the average value. The characteristic length of the minority phase was found to be  $\xi_1 = \xi/(1 - \varphi_1) = 5.1 \text{ nm}$  and the characteristic length of the major phase was  $\xi_2 = \xi/\varphi_1 = 41.8 \text{ nm}$ . This suggests that the inner structure of the copolymer can be described as a continuous copolymer phase, its composition being slightly richer in PBBA, in which domains of pure polystyrene are randomly distributed. The characteristic length of the domains is significantly smaller than the radius of gyration of a polymer chain (about 14 nm for the studied copolymer,  $M_w = 2.5 \times 10^5 \text{ g/g}\cdot\text{mol}$ ). It should be noted that the derivation of the present model assumes a sharp interface between the two phases. This may not be strictly the case for a random copolymer in which a wide distribution of sequence lengths exists. A wide boundary region should result in deviations from an  $h^{-4}$  scaling at large values of  $h$ . This is not observed in the angular region studied.

Although the good fit to the model is an indication to the existence of an irregular inner structure, the possibility that other structural details exist in the particle has to be considered as well. The model predicts that if the structure is "purely" irregular, the cross term will have zero values throughout the whole angular range.

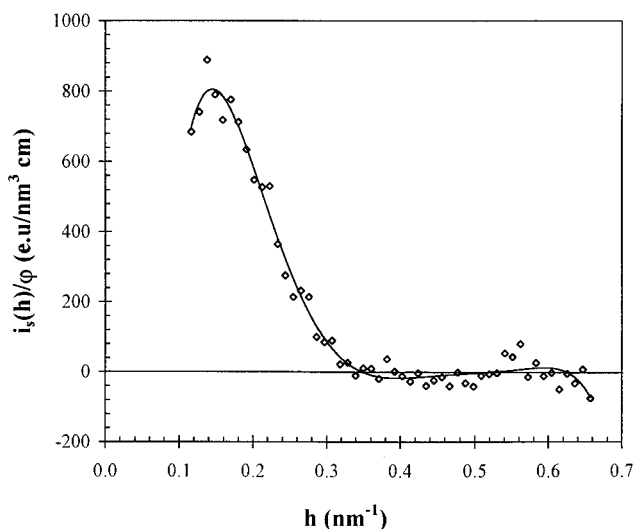


Figure 7. The calculated cross term.

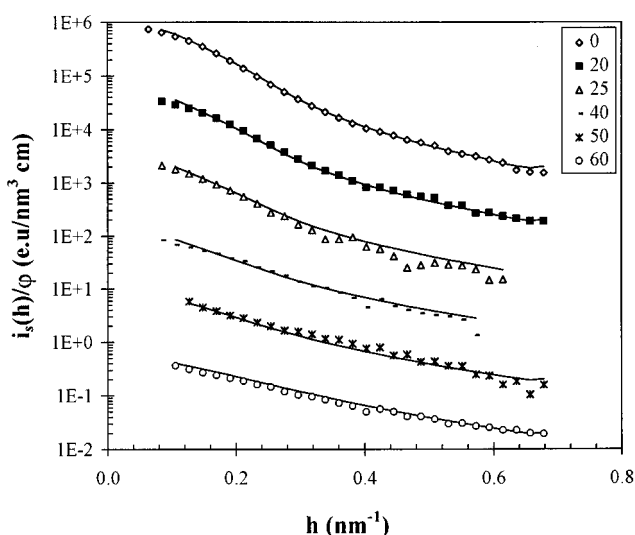


Figure 8. Smeared SAXS scattering intensities obtained at different contrasts. The solid lines were calculated assuming that  $i_{ih}(h) = 0$  for all  $h$  values. Legends indicate weight percentage of sucrose in the solution. For the sake of clarity, the curves were shifted vertically by multiple factors of 10.

As can be seen in Figure 7, this condition is not fulfilled for the studied copolymer. However, the contribution of the cross term to the total scattering intensity is negligible, as shown in Figure 8. The solid lines in this figure were calculated assuming that  $i_{ih}(h) = 0$  for all  $h$  values. The good fit to the experimental data confirms the validity of the assumption. Thus, the deviation of the cross term from zero values is probably a result of the variation in the average composition and hence electron density between the particles, an effect not accounted for in the present model.

## Conclusions

The contrast variation method was shown to be a sensitive probe for inhomogeneity within copolymer latex particles. The separation of the homogeneous function allows direct calculation of the size distribution of the spherical particles. The SAXS analysis reveals an inner structure described by a continuous copolymer phase, its composition being slightly richer in PBBA, in which domains of pure polystyrene are randomly distributed. This quantitative method fully describes the particles' inner structure, including the volume

fraction of the domains and their characteristic length.

## References and Notes

- (1) Poehlein, G. W. *Encyclopedia of Polymer Science and Engineering*; John Wiley & Sons: New York, 1988; Vol. 6, p 1.
- (2) Omi, S.; Kushibiki, K.; Iso, M. *Polym. Eng. Sci.* **1987**, *27*, 470.
- (3) Doughert, E. P. *J. Appl. Polym. Sci.* **1986**, *32*, 3051.
- (4) Lee, K. C.; El-Aasser, M. S.; Vanderhoff, J. W. *J. Appl. Polym. Sci.* **1992**, *45*, 2207.
- (5) Lee, K. C.; El-Aasser, M. S.; Vanderhoff, J. W. *J. Appl. Polym. Sci.* **1992**, *45*, 2221.
- (6) Šnupárek, J., Jr.; Krška, F. *J. Appl. Polym. Sci.* **1977**, *21*, 2253.
- (7) van Doremale, J. H. J.; Schoonbrood, H. A. S.; Kurja, J.; German, A. L.; *J. Appl. Polym. Sci.* **1992**, *45*, 957.
- (8) Stuhmann, H. B.; Kirste, R. G. *Z. Phys. Chem. Frankfurt* **1965**, *46*, 247.
- (9) Feigin L. A.; Svergun D. I. In *Structure Analysis by Small-Angle X-ray and Neutron Scattering*; Plenum Press: New York, 1987.
- (10) Bianco, H.; Narkis, M.; Cohen, Y. Submitted for publication.
- (11) Yuan, Y.; Siegmann, A.; Narkis, M. *J. Appl. Polym. Sci.* **1996**, *60*, 1475.
- (12) Dingenouts, N.; Ballauff, M. *Acta Polym.* **1993**, *44*, 178.
- (13) Stabinger, H.; Kratky, O. *Makromol. Chem.* **1978**, *179*, 1655.
- (14) Guinier, A.; Fournet, G. *Small-Angle Scattering of X-rays*; John Wiley & Sons: New York, 1955.
- (15) Glatter, O.; Kratky, O. *Small Angle X-ray Scattering*; Academic Press: London, 1982.
- (16) Bianco, H.; Narkis, M.; Cohen, Y. *J. Polym. Sci.: Polym. Phys.* **1996**, *34*, 2775.
- (17) Stuhmann, H. B. *J. Appl. Crystallogr.* **1974**, *7*, 173.
- (18) Stuhmann, H. B. *J. Appl. Crystallogr.* **1975**, *8*, 538.
- (19) Philipse, A. P.; Smits, C.; Vrij, A. *J. Colloid Interface Sci.* **1989**, *129*, 335.
- (20) Glatter, O. *Acta Phys. Austriaca* **1977**, *43*, 307.
- (21) Glatter, O. *J. Appl. Crystallogr.* **1977**, *10*, 415.
- (22) Glatter, O. *J. Appl. Crystallogr.* **1980**, *13*, 7.
- (23) Debye, P.; Anderson, H. R.; Brumberger, H. *J. Appl. Phys.* **1957**, *28*, 679.
- (24) Wu, W. *Polymer* **1982**, *23*, 1907.

MA961641A